Biochemistry

 Volume 38, Number 5 February 2, 1999

Accelerated Publications

Identification of a Guanylyl Cyclase-Activating Protein-Binding Site within the Catalytic Domain of Retinal Guanylyl Cyclase1†

Izabela Sokal,‡ Françoise Haeseleer,‡ Anatol Arendt,§ Elinor T. Adman,|| Paul A. Hargrave,§,⊥ and Krzysztof Palczewski*,‡,#

Departments of Ophthalmology, Pharmacology, Chemistry, and Biological Structure, University of Washington, Seattle, Washington 98195; and Departments of Ophthalmology and Biochemistry and Molecular Biology, University of Florida, Gainesville, Florida 32610

Received October 21, 1998; Revised Manuscript Received December 2, 1998

ABSTRACT: Regulation of cAMP and cGMP production is a fundamental step in a broad range of signal transduction systems, including phototransduction. To identify regions within photoreceptor guanylyl cyclase 1 (GC1) that interact with GC-activating proteins (GCAPs), we synthesized the intracellular fragment of GC1, residues 491−1110, as a set of 15 amino acid long, partially overlapping peptides on the surface of individual pins arranged in a microtiter plate format. This pin assay identified 8 peptides derived from different regions of the GC1 intracellular domain that bind GCAPs. Peptide variants containing these sequences were synthesized as free peptides and tested for their ability to inhibit GC1 stimulation by GCAPs. A free peptide,[968]GTFRMRHMPEVPVRIRIG, from the catalytic domain of GC1 was the strongest inhibitor of GCAP1/GCAP2-mediated activation. In native GC1, this polypeptide fragment is likely to form a loop between α-helix 3 and β-strand 4. When this region in GC1 was replaced by the corresponding sequence of GCAP-insensitive GC type A, GCAPs did not stimulate the GC1 mutant. The corresponding loops in related adenylyl cyclase (AC) are involved in the activating and inhibiting interactions with $G_{s\alpha}$ and $G_{i\alpha}$, respectively. Thus, despite interacting with different activating proteins, both AC and GC activity may be modulated through their respective regions within catalytic domains.

The enzymes that catalyze the production of 3′,5′-cyclic AMP (cAMP), 3′,5′-cyclic GMP (cGMP), adenylyl cyclase (AC), and guanylyl cyclase (GC) share a significant degree of sequence homology, particularly in the catalytic domain. Both cyclases catalyze the formation of 3′,5 ′-cyclic purine nucleotide monophosphates from their precursor nucleoside 5′-triphosphates. The reactions proceed by direct in-line attack of the 3′-hydroxyl group of the ribose on the γ-phosphate of the triphosphate nucleotides. The divalent

† This research was supported by grants from NIH EY08061, EY06225, and EY06226, and by an award from Research to Prevent Blindness, Inc. (RPB), to the Department of Ophthalmology at the University of Washington and the University of Florida. K.P. is a recipient of a Jules and Doris Stein Professorship from RPB. E.T.A. is supported in part by UW Center grant number P30 ES07033 from the National Institute of Environmental Health Sciences, NIH.

* Address correspondence to: Krzysztof Palczewski, Ph.D., University of Washington, Department of Ophthalmology, Box 356485, Seattle, WA 98195-6485. Phone: 206-543-9074. Fax: 206-543-4414. E-mail: palczews@u.washington.edu.

‡ Department of Ophthalmology, University of Washington.

§ Department of Ophthalmology, University of Florida.

|| Department of Biological Structure, University of Washington.

⊥ Department of Biochemistry and Molecular Biology, University of Florida.

Departments of Pharmacology and Chemistry, University of Washington.

10.1021/bi982512k CCC: $18.00
Published on Web 01/12/1999

ions, Mg^{2+} or Mn^{2+}, are essential for enzymatic catalysis (*1*−*6*). AC may employ a catalytic mechanism analogous to that of DNA polymerase, in which two Mg^{2+} ions facilitate the nucleophilic attack of the 3′-hydroxyl group and the subsequent elimination of pyrophosphate (*7*). This cyclization is stereospecific with inversion of the configuration on the γ-phosphate group. Each cyclase is highly specific for its corresponding triphosphate nucleotides, and certain mutations within the purine recognition domain can convert one cyclase to another (*8*, *9*). The catalytically competent unit is a dimer formed within one polypeptide chain from two homologous C1 and C2 domains (AC) (*10*) or between domains located on two homo- or hetero-subunits (particulate GC). Multiple forms of ACs and GCs are typically stringently regulated by various independent mechanisms characteristic for AC or GC that involve G proteins, circulating peptides, NO, phosphorylation, and Ca^{2+}-binding proteins such as calmodulin and GC-activating proteins (GCAPs) (*5*, *11*, *12*).

Recently, the crystal structure of a soluble, catalytically active fragment of AC, in a complex with its stimulatory heterotrimeric G protein α-subunit, $G_{s\alpha}$, was determined (*10*). The binding of $G_{s\alpha}$ to AC induces a change in the orientation of the C2 domain, with subsequent changes within the active site promoting catalysis. This reorientation of the C2 domain could result from an insertion of a helix of $G_{s\alpha}$ into a cleft formed by α1-α2 and α3 helices of AC (*10*). Dessauer et al. (*13*) found that $G_{i\alpha}$ binds within the cleft formed by the α2 and α3 helices of C1, resembling the $G_{s\alpha}$ binding site in C2. On the basis of the crystal structure of the AC−C2 homodimer, a model of a heterodimeric soluble GC and a homodimeric membrane GC (*14*) further suggests that the overall topology of the catalytic domains of both cyclases could be similar.

In vision, the concentration of cGMP ([cGMP]) and $[Ca^{2+}]$ within photoreceptor cells decreases as a result of activation of the phototransduction cascade (reviewed in refs *12* and *15*). Restoration of the photoreceptor dark conditions requires activation of particulate GCs (*16*) by Ca^{2+}-free forms of GCAPs (reviewed in ref 12). GCAPs are 23 kDa Ca^{2+}-binding proteins belonging to the calmodulin superfamily. Four forms of photoreceptor GCAPs and two forms of photoreceptor GC have been characterized: GCAP1 (*17*), GCAP2 (*18*, *19*), GCAP3 (*20*), frog-specific GCIP (*21*), GC1 (*22*) and GC2 (*23*). Consistent with the physiology of photoreceptors, GCAPs interact with GC intracellularly (*24*−*26*). However, it is unclear how the interaction with GCAPs stimulates GC activity mechanistically. For example, GCAPs could promote dimerization of GC in a Ca^{2+}-dependent manner, or analogous to the mechanism seen with AC and $G_{s\alpha}$, GCAPs could induce specific conformational changes in GC that result in low or high catalytic efficiency that parallels the changes in $[Ca^{2+}]$. To better understand the mechanism of GC1 activation by GCAPs, we used a peptide approach to identify major interaction sites between these proteins. The results of our studies suggest that AC and GC may be stimulated through interaction of corresponding regions within the catalytic domains with auxiliary proteins.

MATERIALS AND METHODS

Preparation of Rod Outer Segments (ROS). ROS were prepared from fresh bovine retinas (Schenk Packing Co., Inc., Stanwood, WA). Washed ROS were prepared from ROS by removing soluble proteins, including GCAP1 (*18*). Other standard procedures and production of antibodies were described previously (*18*, *27*).

Expression of GCAP1, GCAP2, and GC1 in High Five Insect Cells. GC1, GCAP1, GCAP2, and GCAP1−His_6 were expressed in High Five insect cells as described previously (*18*, *28*). GCAP1 and GCAP1−His_6 were purified by immunoaffinity (*18*) or affinity methods to apparent homogeneity (*28*). Both GCAP1s had similar properties (*28*). The fusion protein GCAP2-GFP, green fluorescent protein fused to the C-terminus of GCAP2, was expressed in insect cells and immunoaffinity purified by a procedure analogous to the purification of GCAP2 (*27*). The construct was made by Dr. Iswari Subbaraya (Baylor College of Medicine). The activity of expressed GC1 was tested in membrane fractions of transfected insect cells.

GC Assays. The GC assays were performed using GTP-α-^{32}P and washed ROS, or using expressed GC1 as described previously (*28*). $[Ca^{2+}]$ was calculated using the computer program Chelator 1.00 (*29*) and adjusted to higher concentrations in some assays by increasing the amount of added $CaCl_2$. Routine assays were carried out at 50 nM $[Ca^{2+}]$.

Synthesis of Pins, Binding and Detection of GCAPs. Peptides corresponding to residues 491−1110 of retGC1 were produced employing a simultaneous peptide synthesis strategy developed by Geysen et al. (*30*), called Multipin Peptide Synthesis and manufactured by Chiron Technologies, Inc. These peptides were synthesized on derivatized polyethylene components arranged in a microtiter plate format. The peptides were 15 amino acids in length with 8 amino acids overlapping intervals covalently bonded to the surface of plastic pins. The first two peptides were ^{491}YCRHRLL-HIQMVSGP and ^{498}HIQMVSGPNKIILTL. A total of 88 peptides were synthesized. After synthesis, the pins were precoated at room temperature with 2% BSA, 0.1% Tween 20, 0.1% sodium azide in 10 mM sodium phosphate, pH 7.2, containing 100 mM NaCl, and washed with 10 mM sodium phosphate, pH 7.2, containing 100 mM NaCl. For screening of the binding to pins, GCAP1 or GCAP2 (1−2 μg in 175 μL per well) in 10 mM sodium phosphate, pH 7.2, containing 100 mM NaCl and 0.05% Tween 20, was added to each well and incubated for 1 h at room temperature. Pins were washed 3 times with 10 mM sodium phosphate, pH 7.2, containing 100 mM NaCl and 0.05% Tween 20. Monoclonal antibodies, G2 (anti-GCAP1; 0.3 μg/well) or A1 (anti-GCAP2; 0.3 μg/well), were added to each well and incubated for 1 h at room temperature. Pins were washed 3 times with 10 mM sodium phosphate, pH 7.2, containing 100 mM NaCl and 0.05% Tween 20. Anti-mouse alkaline phosphatase conjugate (Bio-Rad), diluted 2000 times, was added to each well and incubated for 1 h at room temperature. Pins were washed three times with 10 mM sodium phosphate, pH 7.2, containing 100 mM NaCl and 0.05% Tween 20. A chromogenic substrate of alkaline phosphatase (*p*-nitrophenyl phosphate in diethanolamine) was added, and the reaction was carried out at pH 9.8 for 1.5 min. The absorption at 405 nm was measured by ELISA reader (Dynatech MR650). To regenerate pins, the plate was sonicated in a water bath (Branson 1200) with 0.1 M potassium phosphate buffer, pH 7.2, containing 1% SDS and 0.1% 2-mercaptoethanol at 60 °C for 10 min. Next, the block was rinsed with deionized

Table 1. Influence of Synthetic Peptides Corresponding to the Intracellular Domain of GC1 on the GC1 Activity Stimulated by GCAP1[a]

Peptide	Sequence	pKa	IC_{50} (μM)
Peptide 11′	^{547}**IHSQLPDYTNIGLYE**GDWVWLKKF	5.4	980
Peptide 25′	^{641}IKLD**WMFKSSLLLDLIKGI**R	9.7	420
Peptide 35′	^{715}**APELLRDPVLERRGT**LAGDVFS	4.7	>2000
Peptide 61′	^{893}GFTT**ISAMSEPIEVVDLLN**DLYT	3.4	420;760***
Peptide 71′	^{968}G**TFRMRHMPEVPVRIR**IG	12	290;120***
Peptide 71a*	~~~~~~~~~~~~~~~~~~**RMRHMPEVPVRIR**IG~~~~~~~~~~~~~~~~		610
Peptide 71b	~~~~~~~~~~~~~~~~~~~~**HMPEVPVRIR**IG~~~~~~~~~~~~~~~~		315
Peptide 71c**	~~~~~~~~~~~~~~~~~~~~~~~~**EVPVRIR**IG~~~~~~~~~~~~~~~~		ND
Peptide 71d**	~~~~~~~~~~~~~~~G**TFRMRHMPEVPVRI**~~~~~~~~~~~~~~~~~~		ND
Peptide 71e**	~~~~~~~~~~~~~~~G**TFRMRHMPEV**~~~~~~~~~~~~~~~~~~~~~~		ND
Peptide 71f**	~~~~~~~~~~~~~~~G**TFRMR**~~~~~~~~~~~~~~~~~~~~~~~~~~~		ND
Peptide 71g	~~~~~~~~~~~~~~~~~~**RMRHMPEVPVRIR**IG~~~~~~~~~~~~~~~~		540
Peptide 71h*	~~~~~~~~~~~~~~~~~~**RMRHMPEVPVRIR**~~~~~~~~~~~~~~~~~~		no effect
Peptide 71k*	~~~~~~~~~~~~~~~~~~~~**RHMPEVPVRIR**~~~~~~~~~~~~~~~~~~		no effect
Peptide 71m	~~~~~~~~~~~~~~~~~~**RMRHMPEVPV**~~~~~~~~~~~~~~~~~~~~~~		no effect
Peptide 83′*	^{1051}**KGKGAEETYWLVGRR**GF~~~~~~~~~~~~~~~~~~~~~~~~~~~~~~~~	6.2	440
Peptide 85′	~~~~~~~~~~~~~~~~^{1067}FN**KPIPKPPDLQPGASN**~~~~~~~~~~~~~~~	8.6	no effect
Peptide 89′	~~~~~~~~~~~~~~~~~~~~~~~~~~~~~~~~^{1084}**HGISLHEIPPDRRQK**	7.0	no effect
Peptide 90′	^{1093}**DRRQKLEKARPGQFS**GK(stop)	11	no effect

[a] The effect of synthetic peptides on GC1 activity was measured in the presence of 1 μM GCAP1 in standard assay conditions as described in Materials and Methods. IC_{50} has been determined from 5−8 concentrations of the peptide. The titration was performed in duplicate. The common sequences with the parental peptides are shown in bold; *, limited solubility (<0.5 mM); **, insoluble in aqueous solutions; ***, GCAP2 instead of GCAP1; ND, not determined due to poor solubility.

water, preheated to 60 °C for 30 s, and shaken in deionized water at 60 °C for 30 min. The plate was then immersed in methanol at 60 °C for 15 s and air-dried.

Bulk Peptide Synthesis. Solid-phase peptide synthesis was performed at the 0.25 mmol level on an automatic peptide synthesizer (Applied Biosystems model 431A) using Fmoc, DCC/HOBt protocol from the ABI manual. Crude peptides were loaded onto a Sephadex G-10 column (2 × 90 cm) equilibrated in 50% acetic acid. The column was developed with 50% acetic acid, and the peptide was detected in the fractions by spotting aliquots of each fraction with fluorescamine. All peptides that inhibited GC/GCAP interaction were further purified by preparative HPLC using a Waters model 600E, equipped with 2.5 × 25 cm Partisil-10 ODS-3 column (Whatman). Elution was performed with a linear gradient from 0.1% aqueous acetic acid (A) to 40% or 50% B (0.1% acetic acid in CH_3CN) over 40 min at 10 mL/min, with the eluent monitored at 230 nm. A Perseptive Biosystems Vestec Voyager RP mass spectrometer with a 337 nm laser was used to analyze peptides using matrix-assisted laser desorption mass spectroscopy. All peptides had a correct amino acid composition determined by acid hydrolysis with 6 N HCl, followed by amino acid analysis. The concentrations of peptides were determined by amino acid analysis.

Affinity Chromatography of GCAPs on Peptide 71 Coupled to CNBr−Sepharose. Soluble extracts containing GCAP1 or GCAP2-GFP were prepared from a 15 cm tissue culture plate of High Five insect cells expressing GCAP1 or GCAP2-GFP using 1 mL of water containing 1 mM benzamidine. The extract was separated from membrane particles by centrifugation (95000*g* for 10 min) and loaded onto a peptide 71-Sepharose column. The column was prepared according

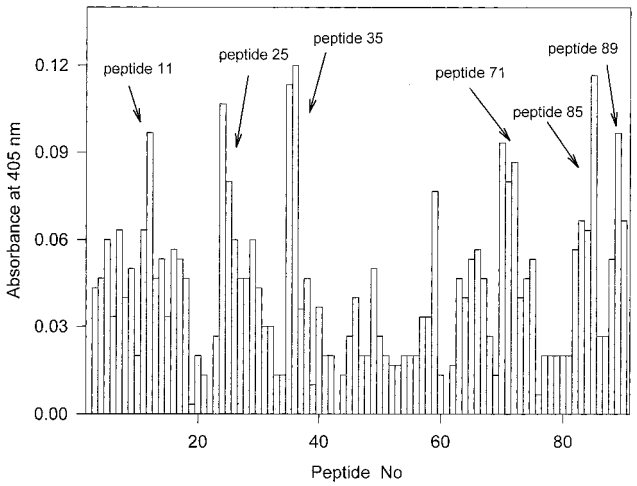

FIGURE 1: *Binding of GCAP1 to the peptide library corresponding to residues 491−1110 of the intracellular domain of retGC1.* Peptides (15 amino acids long with overlapping intervals every 8 aa) were synthesized on polyethylene pins arranged in a microtiter plate format. They were screened simultaneously for binding of GCAPs using anti-GCAP antibodies and an ELISA (see Materials and Methods). The sequence of selected peptides is given in Table 1. These results represent an average of three experiments.

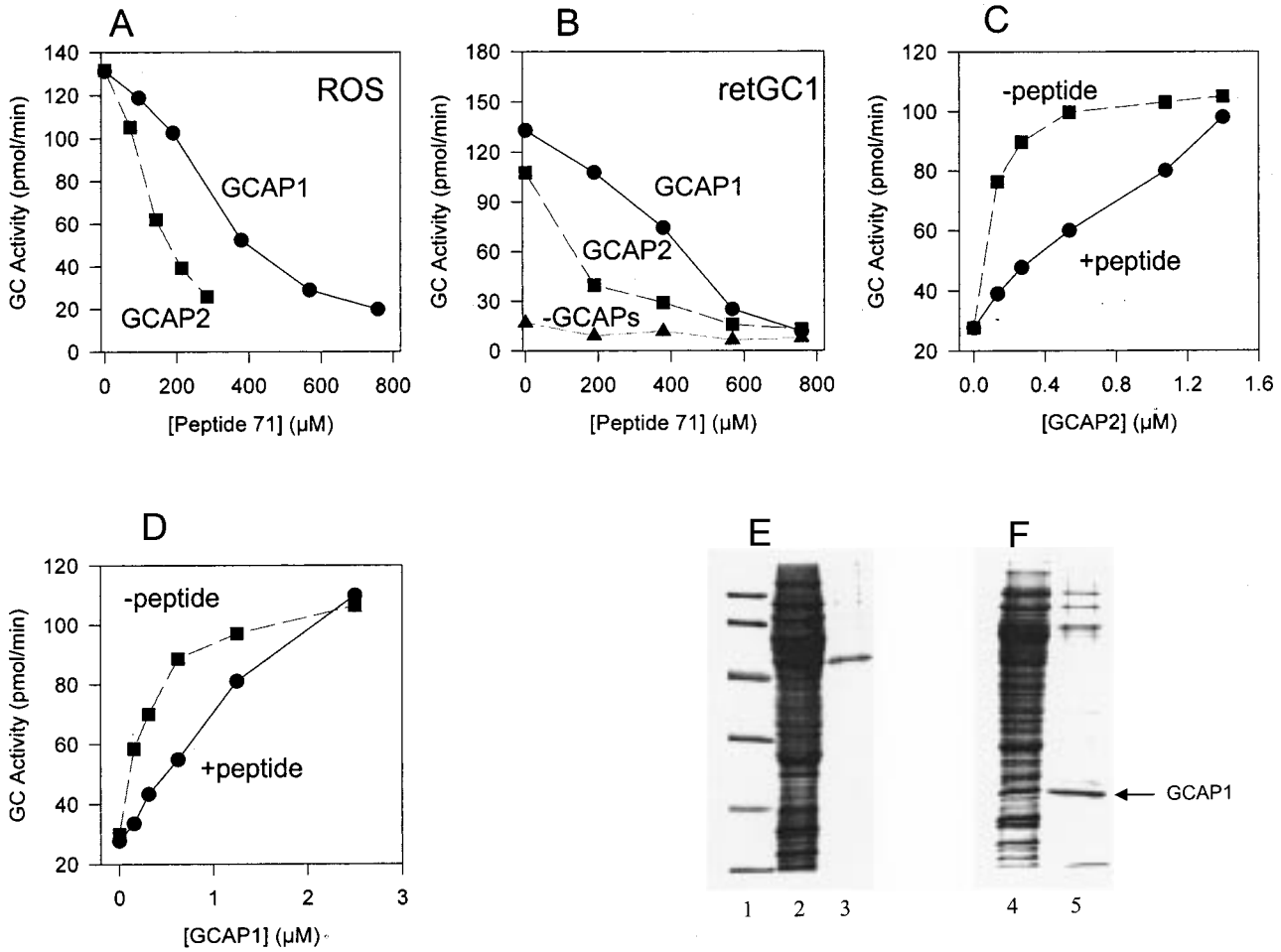

FIGURE 2: *Interaction of peptide 71 with GCAP1 or GCAP2.* (**A**) Dose-dependent inhibition of GC activity in washed ROS suspension at 50 nM [Ca^{2+}] by peptide 71 in the presence of 1 μM GCAP1 or GCAP2. (**B**) Dose-dependent inhibition of recombinant GC in insect cell membrane suspension at 50 nM [Ca^{2+}] by peptide 71 in the presence of 1 μM GCAP1 or GCAP2. (**C**) Dose-dependent activation of GC activity in washed ROS suspension at 50 nM [Ca^{2+}] by GCAP2-GFP in the presence or absence of 300 μM peptide 71. (**D**) Dose-dependent activation of GC activity in washed ROS suspension at 50 nM [Ca^{2+}] by GCAP1 in the presence or absence of 300 μM peptide 71. (**E**) Binding of GCAP2-GFP and GCAP1 (**F**) to peptide 71 coupled to CNBr−Sepharose. GCAPs were extracted from insect cells and loaded onto the column (Materials and Methods). An aliquot from the eluted fractions was used to test for GC stimulation activity at 50 nM [Ca^{2+}]. Fractions with the highest activity were analyzed using SDS−PAGE: lane: 1, protein standards from the top 92, 67, 43, 30, 23, 14 kDa; lanes 2,4, loaded material; lanes 3,5 eluted fractions. GCAP2-GFP and GCAP1 were identified by Western blotting. Similar results were obtained in three independent experiments for all panels.

to the manufacturer's instructions (3 mg of peptide/1 mL of CNBr-activated Sepharose, Pharmacia) and equilibrated with 10 mM BTP (bis[2-hydroxyethyl]iminotris[hydroxymethyl]-methane), pH 7.5. The column was washed at a flow rate of 15 mL/h with 10 mM BTP, pH 7.5, containing 1 M NaCl (~20 mL) until absorption at 280 nm was <0.08. GCAPs were eluted with 0.1 M glycine/HCl, pH 2.5, and immediately neutralized with 100 μL of 1 M Tris/HCl, pH 8.4. Their GC stimulating activity was measured in 50 nM [Ca^{2+}].

Mutagenesis of Human GC1. Wild-type retGC1 cloned in pRC−CMV (Invitrogen) was obtained from Dr. J. Hurley. The mutation was introduced in retGC1 by amplification with primer FH302 5′CATATGCCC/CAGGAACAACTCAGAC-TG/CGCATAGGCCTGCACTCGGG3′ (*Nde*I/GCA/retGC1−2926−2945)] and primer FH303 [5′TCAAGAGAACTG-GCCCGGCC3′ (bp 3312 (Stop)-3293] using pRC-CMV-GC1. After being heated at 94 °C for 5 min, the reaction was cycled 35 times through 94 °C for 30 s, 65 °C for 30 s, and 68 °C for 2 min with Expand High Fidelity PCR System (Boehringer Mannheim). The PCR product was cloned in pCRII-TOPO vector (Invitrogen) and sequenced by dyedeoxy-terminator sequencing (ABI-Prism, Perkin-Elmer). The mutated GC1 fragment was introduced in retGC1 by ligation of a fragment *Hind*III-*Nde*I (1−2900) with a fragment *Nde*I-*Nar*I (2901−3146) covering the mutation and a fragment *Nar*I-*Xba*I (3147−3548) in pRC−CMV opened by *Hind*III-*Xba*I.

Expression in HEK293 Cells. Twenty micrograms of the vector, pRC-CMV-GC1 or pRC-CMV-mutant GC1, was transiently transfected into 50−80% confluent HEK293 cells using coprecipitates of calcium phosphate and DNA (*31*). After 72 h, the cells were washed with phosphate-buffered saline (PBS) and collected in PBS, 0.5 mM EDTA.

Model of AC and GC. Coordinates for the AC/$G_{s\alpha}$ structure (1AZS.pdb) and the GC homology model (1AWN.pdb) were obtained from the Protein Data Bank (*32*). The GC homology model consists of a heterodimer, constructed from the sequence of CYG1_BOVIN (P16068) for chain B, and CYG3_BOVIN (P19687) for chain A (*14*). 1AWN.pdb chain A was superposed visually using the program O (*33*) on chain B of 1azs.pdb, which resulted in GTP of the GC model

FIGURE 3: *Sequence alignment of peptide 71 with selected GCs and AC−V.* Within the sequence corresponding to peptide 71, letters in red represent changes as compared with human GC1; outside this sequence, letters in green represent conserved amino acids among compared sequences (V = L = I; S = T). The yellow boxes below the sequences represent β-strands 3 and 4, the green box represents α-helix 3 in the crystal structure of AC (*10*). The sequences were obtained from GenBank. Accession numbers were for human GC1 (hGC1) Q02846; bovine GC1 (bGC1) O02809; mouse GC1 (mGC1) P52785; rat GC1 (rGC1) P51840; rat GC2 (rGC2) P51842; human GC2 (hGC2) P51841; olfaction rat GC (olf-rGC) P51839; human GC-A (GC-A) P16066; human GC−B (GC−B) P20594; human GC−C (GC−C) P25092; rat AC−V (rAC−V) Q04400; and the β-chain of soluble bovine GC (sol-GC) P16068.

superposing reasonably well with the forskolin analogue in the AC structure. The alignment:

```
hGC1 HAAEI ANMSL DILSA VGTFR MRHMP EVPVR IRIGL HSG
CYG3 HAVQI ALMAL KMMEL SHEV- -PH-G E-PIK MRIGL HSG
                xxx xxxxx xx
```

was used to superimpose helix 3 and strand 4. xxx represents the loop region that was modeled; HA starts helix 3, and HSG ends strand 4. The hyphens indicate insertions relative to the CYG3 model. A rough model of the loop region between helix 3 and strand 4 was constructed by moving another loop region having four additional residues and running through several iterations of the command "lego loop" in "O", which presents the C-alpha traces of the twenty nearest matching loops from a database of structures and allows one to choose a suitable match. Since the purpose was to merely show a likely direction for the inserted loop, the final coordinates were not energy minimized, nor is the modeled loop entirely satisfactory.

RESULTS AND DISCUSSION

Binding of GCAP1 to the Peptide Library Corresponding to the Intracellular Domain of retGC1. Overlapping peptides from the entire intracellular domain of human GC1 (residues 491−1110) were synthesized on pins in a microtiter plate format. Fifteen amino acid long peptides were attached by an uncleavable bond to polyethylene rods in each well (15 nmol/well). These peptides were incubated with 1−2 μg of either purified GCAP1 or fluorescently tagged GCAP2, GCAP2-GFP, with GFP fused to the C-terminus. GCAP2-GFP exhibited properties that were indistinguishable from native GCAP2 in affinity for GC1 and Ca^{2+} sensitivity, but its expression level in insect cells was significantly elevated as compared to wild-type (wt) GCAP2 (Subbaraya and Palczewski, unpublished). Unbound GCAPs were washed off with a buffer containing 100 mM NaCl. Next, the pins were probed with anti-GCAP monoclonal antibodies and then with the secondary anti-IgG antibody conjugated with alkaline phosphatase. The peptide−GCAP−anti-GCAP−anti-IgG complex was detected with an alkaline phosphatase substrate and quantified by spectrophotometry.

GCAP1 and GCAP2-GFP bound with highest affinity to a subset (**11**, **25**, **35**, **71**, **83**, **85**, **89**, and **90**) of the same peptides at low and high [Ca^{2+}] (Figure 1). These observations are consistent with previously published data that GCAPs bind to GC with micromolar affinity in both Ca^{2+}-free and Ca^{2+}-bound forms, leading to respective activation or inhibition of GC1 (*28*, *34*). The effector binding site on GC1 may be similar, if not identical, for GCAP1 and GCAP2 (*18*, *28*). An unrelated GC activator, S-100b, was bound to a different set of peptides than GCAPs (data not shown).

Peptide Inhibition of GC-GCAP Interaction. Peptides of different lengths that contained sequences encompassing peptides **11**, **25**, **35**, **71**, **83**, **85**, **89**, and **90** were synthesized as free peptides (denoted by ′). The inhibitory effects of these peptides on GCAP1/2-stimulated cGMP production were tested in reconstitution assays using washed rod outer segments (ROS) as a source of GCs as described in Materials and Methods. Peptides **25′**, **71′**, and **83′** inhibited ROS-GC1 stimulation by GCAP1 (Table 1). Among these peptides, peptide **71′** was the most potent, with an IC_{50} = 290 μM for GCAP1 and IC_{50} = 120 μM for GCAP2 (Table 1) and was selected for more detailed analyses. In our assay, highly charged peptides from the C-terminal region of GC1 (peptides **85′**, **89′**, and **90′**) did not inhibit cGMP production.

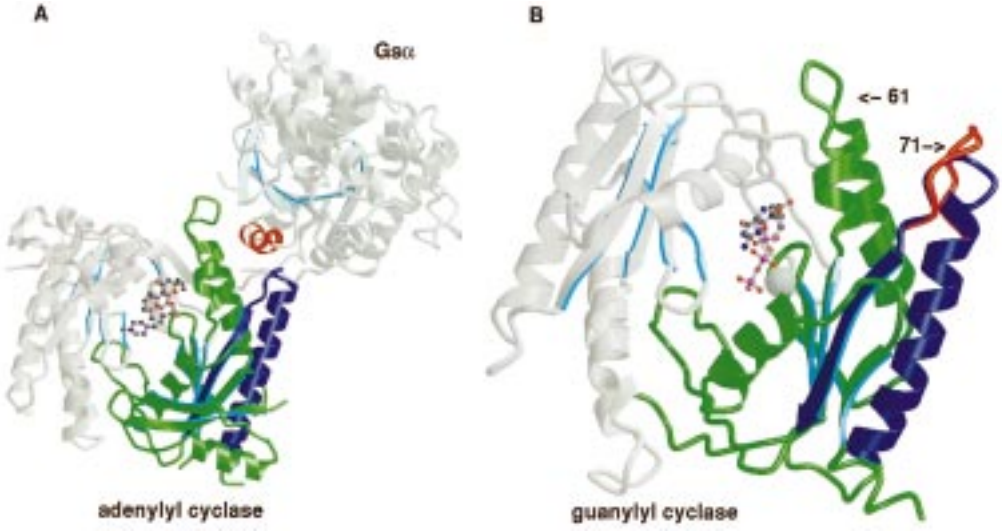

FIGURE 4: *Model of AC and GC.* (**A**) The crystal structure of the VC1 and IIC2 domains of AC complexed with $G_{s\alpha}$ with its interacting helix colored red, and the forskolin analogue (7-deacetyl-7-(*O*-*N*-methylpiperazine)-*g*-butyryl forskolin) shown as ball-and-stick [PDB code 1azs, (*10*)]. (**B**) GC model [PDB code 1awn, (*14*)] in the same orientation, with the newly modeled loop of hGC1 shown in red (peptide 71). GTP is shown as ball-and-stick and Mg^{2+} as a gray ball. In A and B, helix α3 and strand β4 are highlighted in blue, and the rest of that domain is in green. The other domain of the catalytic domain pair is gray. The figure was made using MOLSCRIPT (*38*) and RASTER3D (*39*).

The specificity of peptide **71′** was further tested by synthesis of several truncated peptides. Truncation of the N-terminal region of the peptide and extension at the C-terminal region initially had a modest decreasing effect on the inhibitory properties of these peptides, but removal of HMP sequence decreased peptide solubility. Truncation of the C-terminus and extension at the N-terminus also led to poor solubility of these peptides. When the peptide was truncated at the N-terminus to RMRHMPEVPVRIRIG, it still retained inhibitory properties. C-terminal truncation eliminated the inhibitory properties of the peptide (Table 1).

Peptide **71′** demonstrated significant inhibition of GC1 stimulation by GCAP2. Peptide **71′** inhibited the stimulation of GC(s) in ROS by GCAP2 (IC_{50} = 120 μM) more potently than GCAP1 − GC1 (IC_{50} = 290 μM) (Figure 2A), but had no influence on the basal cyclase activity (data not shown). Similarly, peptide **71′** inhibited stimulation of recombinant GC1 (Figure 2B). Lack of inhibition of the basal cyclase activity and recovery of the stimulation by GCAPs when used in excess (Figure 2C and 2D) suggest that peptide **71′** binds to GCAP rather than to GC. This idea is supported by experiments with peptide **71′**-Sepharose (Figure 2E, 2F). From a complex extract of GCAPs from transfected insect cells which contained many proteins (or retina, data not shown), GCAP1 and GCAP2-GFP were selectively enriched on the immobilized peptide. GCAP1 and GCAP2-GFP were then selectively eluted at low pH. In control experiments, an unrelated GC activator, S100b, and proteins from uninfected insect cell extracts did not bind the peptide **71′**-Sepharose.

Inactivation of GCAP-Dependent Stimulation of GC1. The catalytic domains of particulate GCs, AC, and soluble GC are homologous. However, the homology within the region that corresponds to peptide **71′** is highly conserved only among GCAP-activated GCs, GC1 and GC2. In addition, olfactory GC (olf-GC) which may be GCAP-stimulated (*35*), also shows a high degree of homology in this region (Figure 3). According to a homology model for GC1 (ref *14*; Figure 4), the sequence of peptide **71′** corresponds to a loop formed between α-helix-3 and β-strand 4. A GC1 mutant was made which had the ^{970}EVPVRI sequence replaced with the corresponding sequence within GC-A, QEQLRL. The expression levels of both GC1 and the mutant were comparable (by a factor of 2) as judged by the basal activity of GCs and

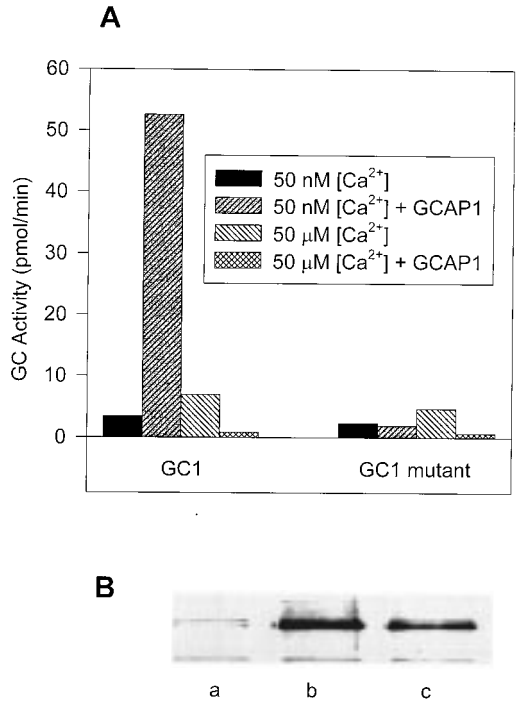

FIGURE 5: *Effect of GCAP1 on activities of GC1 and its mutant.* (**A**) Membranes from HEK293 cells containing recombinant GC1 or its mutant were reconstituted with GCAP1 at 50 nM [Ca^{2+}] or 50 μM [Ca^{2+}]. The basal activity (1−2 pmol/min) of control, untransfected cells was subtracted. Similar results were obtained from 5 independent transfections. (**B**) Expression levels of GC1 (b) and its mutant (c) in HEK cells as analyzed by Western blot using UW28 pAb. The expression level differed by a factor of 2 (taken into account for the GC assays). No immunoreactive band was detected in control cells (a).

by Western blot (Figure 5B). The native form of GC1 was stimulated by the Ca^{2+}-free form of GCAP1, while the GC1 mutant was not activated in our experimental conditions (Figure 5A). Both GC1 and its mutant were inhibited at high $[Ca^{2+}]_{free}$ by GCAP1. Since this sequence forms a loop in GCs that is not directly adjacent to the active site, this mutation is likely to have only a small effect on the overall structure of the active site, consistent with its observed high basal activity (Figure 5A).

The second part of the interacting cleft is formed by a loop encompassing peptide **61′** (Figure 4). In the GC assay, peptide 61′ showed significant inhibition of GC1 stimulation by GCAPs (Table 1). The parental peptide **61** has not been identified in our initial search, likely due to its inadequate length.

CONCLUSIONS

The most interesting observation from this study is that the inhibitory peptide **71′** of GC1-GCAP interaction corresponds to one of the loops of AC that was shown to be involved in contact with $G_{s\alpha}$ (*10*). This interaction with $G_{s\alpha}$ ultimately leads to the activation of AC. Skiba and Hamm (*36*) proposed that $G_{s\alpha}$ is an allosteric regulator of AC that stabilizes the transition state of the substrate. In addition to peptide **71′**, peptide **61′** also displays inhibitory properties preventing GC stimulation by GCAPs. Peptide **61′** corresponds to the same region of the catalytic domain of GC forming a cleft with the loop which contains the peptide **71′** sequence, to which GCAPs may dock. In fact, peptide **61′** corresponds to the α1-α2 loop in AC, which forms the part of AC that binds $G_{s\alpha}$ (Figure 4). Anchoring GCAPs to GC involves multiple areas, including the kinase-like domain (*24*, *37*). In this study we identified a new region within the catalytic domain that may be critical for GC activation. GCAPs, like $G_{s\alpha}$ in the AC system, may stabilize (in Ca^{2+}-free state) the GC transition state with GTP. A high-resolution crystal structure of GCAPs with GC will be needed to definitively answer if the activation of retinal GCs by GCAPs is mechanistically similar to the activation of AC by $G_{s\alpha}$. These studies point to such a possibility.

ACKNOWLEDGMENT

We would like to thank Dr. Iswari Subbaraya (Baylor College of Medicine) for GCAP2-GFP, Dr. James B. Hurley and Richard Laura (University of Washington) for the GC1 clone, and John W. Crabb (Cleveland Clinic Foundation) for the amino acid analysis.

REFERENCES

1. Gerlt, J. A., Coderre, J. A., and Wolin, M. S. (1980) *J. Biol. Chem. 255*, 331−334.
2. Eckstein, F., Romaniuk, P. J., Heideman, W., and Storm, D. R. (1981) *J. Biol. Chem. 256*, 9118−9120.
3. Senter, P. D., Eckstein, F., Mulsch, A., and Bohme, E. (1983) *J. Biol. Chem. 258*, 6741−6745.
4. Krupinski, J. (1991) *Mol. Cell. Biochem. 104*, 73−79.
5. Garbers, D. L., Koesling, D., and Schultz, G. (1994) *Mol. Biol. Cell. 5*, 1−5.
6. Hobbs, A. J. (1997) *Trends Pharmacol. Sci. 18*, 484−491.
7. Zimmermann, G., Zhou, D., and Taussig R. (1998) *J. Biol. Chem. 273*, 19650−19655.
8. Tucker, C. L., Hurley, J. H., Miller, T. R., and Hurley, J. B. (1998) *Proc. Natl. Acad. Sci. U.S.A. 95*, 5993−5997.
9. Sunahara, R. K., Beuve, A., Tesmer, J. J. G., Sprang, S. R., Garbers, D. L., and Gilman, A. G. (1998) *J. Biol. Chem. 273*, 16332−16338.
10. Tesmer, J. J. G., Sunahara, R. K., Gilman, A. G., and Sprang, S. R. (1997) *Science 5345*, 1907−1916.
11. Sunahara, R. K., Dessauer, C. W., and Gilman, A. G. (1996) *Annu. Rev. Pharmacol. Toxicol. 36*, 461−480.
12. Polans, A. S., Baehr, W., and Palczewski, K. (1996) *Trends Neurosci. 19*, 547−554.
13. Dessauer, C. W., Tesmer, J. J. G., Sprang, S. R., and Gilman, A. G. (1998) *J. Biol. Chem. 273*, 25831−25839.
14. Liu, Y., Ruoho, A. E., Rao, V. D., and Hurley, J. H. (1997) *Proc. Natl. Acad. Sci. U.S.A. 94*, 12414−12419.
15. Koutalos, Y., and Yau, K.-W. (1996) *Trends Neurosci. 19*, 73−81.
16. Koch, K. W., and Stryer, L. (1988) *Nature 334*, 64−66.
17. Palczewski, K., Subbaraya, I., Gorczyca, W. A., Helekar, B. S., Ruiz, C. C., Ohguro, H., Huang, J., Zhao, X., Crabb, J. W., Johnson, R. S., Walsh, K. A., Gray-Keller, M., Detwiller, P., and Baehr, W. (1994) *Neuron 12*, 395−404.
18. Gorczyca, W. A., Polans, A. S., Surgucheva, I. G., Subbaraya, I., Baehr, W., and Palczewski, K. (1995) *J. Biol. Chem. 270*, 22029−22036.
19. Dizhoor, A. M., Olshevskaya, E. V., Henzel, W. J., Wong, S. C., Stults, J. T., Ankoudinova, I., and Hurley, J. B. (1995) *J. Biol. Chem. 270*, 25200−25206.
20. Haeseleer, F., Sokal, I., Li, N., Pettenati, M., Rao, N., Bronson, D., Wechter, R., Baehr, W., and Palczewski, K. (1998) *J. Biol. Chem.* (in press).
21. Li, N., Fariss, R. N., Zhang, K., Otto-Bruc, A., Haeseleer, F., Branson, D., Qin, N., Yamazaki, A., Subbaraya, I., Milam, A. H., Palczewski, K., and Baehr, W. (1998) *Eur. J. Biochem. 252*, 591−599.
22. Shyjan, A. W., de-Sauvage, F. J., Gillett, N. A., Goeddel, D. V., and Lowe, D. G. (1992) *Neuron 9*, 727−737.
23. Lowe, D. G., Dizhoor, A. M., Liu, K., Gu, Q., Spencer, M., Laura, R., Lu, L., and Hurley, J. B. (1995) *Proc. Natl. Acad. Sci. U.S.A. 92*, 5535−5539.
24. Duda, T., Goraczniak, R., Surgucheva, I., Rudnicka-Nawrot, M., Gorczyca, W. A., Palczewski, K., Sitaramayya, A., Baehr, W., and Sharma, R. K. (1996) *Biochemistry 35*, 8478−8482.
25. Laura, R. P., Dizhoor, A. M., and Hurley, J. B. (1996) *J. Biol. Chem. 271*, 11646−11651.
26. Krishnan, A., Goraczniak, R. M., Duda, T., and Sharma, R. K. (1998) *Mol. Cell. Biochem. 178*, 251−259.
27. Otto-Bruc, A., Buczylko, J., Surgucheva, I., Subbaraya, I., Rudnicka-Nawrot, M., Crabb, J. W., Arendt, A., Hargrave, P. A., Baehr, W., and Palczewski, K. (1997) *Biochemistry 36*, 4295−4302.
28. Rudnicka-Nawrot, M., Surgucheva, I., Hulmes, J. D., Haeseleer, F., Sokal, I., Crabb, J. W., Baehr, W., and Palczewski, K. (1998) *Biochemistry 37*, 248−257.
29. Schoenmakers, T. J., Visser, G. J., Flik, G., and Theuvenet, A. P. (1992) *BioTechniques 12*, 870−874.
30. Geysen, H. M., Meloen, R. H., and Barteling, S. J. (1984) *Proc. Natl. Acad. Sci. U.S.A. 81*, 3998−4002.
31. Sambrook, J., Fritsch, E. F., and Maniatis, T. (1989) *Molecular Cloning, A laboratory manual*, 2nd ed., Cold Spring Harbor Lab Press, Plainview, NY.
32. Bernstein, F. C., Koetzle, T. F., Williams, G. J. B., Meyer, E. F., Bruce, M. D., Rodgers, J. R., Kennard, O., Shimanouchi, T., and Tasmui, M. (1977) *J. Mol. Biol. 112*, 535−542.
33. Jones, T. A., Zou, J.-Y., Cowan, S. W., and Kjeldgaard, M. (1991) *Acta Crystallogr. Sect. A 47*, 110−119.
34. Dizhoor, A. M., and Hurley, J. B. (1996) *J. Biol. Chem. 271*, 19346−19350.
35. Moon, C., Jaberi, P., Otto-Bruc, A., Baehr, W., Palczewski, K., and Ronnett, G. V. (1998) *J. Neurosci. 18*, 3195−3205.
36. Skiba, N. P., and Hamm, H. E. (1998) *Nat. Struct. Biol. 5*, 88−92.
37. Laura, R. P., and Hurley, J. B. (1998) *Biochemistry 37*, 11264−11271.
38. Kraulis, P. (1991) *J. Appl. Crystallogr. 24*, 946−950.
39. Merritt, E. A., and Murphy, M. E. P. (1994) *Acta Crystallogr., Sect. D 50*, 869−873.

BI982512K